Inorg. Chem. **2005**, *44*, 225–231

Laser Photoinitiated Nitrosylation of 3-Electron Reduced *Nm europaea* Hydroxylamine Oxidoreductase: Kinetic and Thermodynamic Properties of the Nitrosylated Enzyme

Maria Zulema Cabail, Joshua Kostera, and A. Andrew Pacheco*

Department of Chemistry, University of Wisconsin—Milwaukee, Milwaukee, Wisconsin 53211

Received August 25, 2004

Hydroxylamine-cytochrome *c554* oxidoreductase (HAO) catalyzes the 4-e$^-$ oxidation of NH_2OH to NO_2^- by cytochrome *c554*. The electrons are transferred from NH_2OH to a 5-coordinate heme known as P_{460}, the active site of HAO. From P_{460}, *c*-type hemes transport the electrons through the enzyme to a remote solvent-exposed *c*-heme, where cyt *c554* reduction occurs. When 3–60 μM NO$^\bullet$ are photogenerated by laser flash photolysis of *N,N*′-bis-(carboxymethyl)-*N,N*′-dinitroso-1,4-phenylenediamine, in a solution containing $\sim$1 μM HAO prereduced by 3 e$^-$/subunit, the HAO *c*-heme pool is subsequently oxidized by up to 1 e$^-$/HAO subunit. The reaction rate for HAO oxidation shows first-order dependence on [HAO], and zero-order dependence on [NO$^\bullet$] ($k_{obs} = 1250 \pm 150$ s^{-1}). However, the total HAO oxidized shows hyperbolic dependence on [NO$^\bullet$]. We suggest that NO$^\bullet$ first binds reversibly to P_{460} giving a {Fe(NO)}^{6} moiety. Intramolecular electron transfer (IET) from the *c*-heme pool then reduces P_{460} to {Fe(NO)}.^{7} The overall binding constant (K) for formation of {Fe(NO)}^{7} from free NO$^\bullet$ and 3-e$^-$ reduced HAO was measured at $(7.7 \pm 0.6) \times 10^4$ M^{-1}. This value is larger than that for typical ferriheme proteins ($\sim 10^4$ M^{-1}), but much smaller than that for the corresponding ferroheme proteins ($\sim 10^{11}$ M^{-1}). The final product generated by nitrosylating 3-e$^-$ reduced HAO is believed to be the same species obtained by adding NH_2OH to the fully oxidized enzyme. The experiments described herein suggest that when NH_2OH and HAO first react, only two of the NH_2OH electrons end up in the *c*-heme pool. The other two remain at P_{460} as part of an {Fe(NO)}^{7} moiety. These results are discussed in relation to earlier studies that investigated the effect of putting fully oxidized and fully reduced HAO under 1 atm of NO$^\bullet$.

Introduction

Nm europaea is a chemolithotrophic bacterium that obtains all its energy from the aerobic oxidation of NH_4^+ to NO_2^-.[1,2] This net oxidation of NH_4^+ to NO_2^- forms a part of the biosphere's nitrogen cycle, and as such has enormous economic and ecological importance.[2−9] Hydroxylamine cytochrome c_{554} oxidoreductase (HAO) catalyzes the 4-e$^-$ oxidation of NH_2OH to NO_2^- by cytochrome c_{554} (cyt c_{554}), which is a critical step in *Nm europaea*'s respiratory process.[2−5] HAO is chemically intriguing because of its complexity: it is a homotrimer with a molecular weight of 204 kDa that contains a total of 24 hemes (Figure 1).[10] Our long-term goal is to shed light on how the complex design features of HAO relate to its function in the *Nm europaea* energy transduction system. One approach to this problem has been to develop a series of novel pulsed-laser techniques for photogenerating putative intermediates of HAO's catalytic

* To whom correspondence should be addressed. E-mail: apacheco@uwm.edu.

(1) Ferguson, S. J. *Curr. Opin. Chem. Biol.* **1998**, *2*, 182−193.
(2) Hooper, A. B. In *Autotrophic Bacteria*; Schlegel, H. G., Bowien, B., Eds.; Science Tech Publishers: Madison, WI, 1989; pp 239−265.
(3) Kroneck, P. M. H.; Beuerle, J.; Schumacher, W. In *Metal Ions in Biological Systems*; Sigel, H., Sigel, A., Eds.; Marcel Dekker Inc.: New York, 1992; pp 455−505.
(4) Wood, P. M. In *The Nitrogen and Sulfur Cycles*; Cole, J. A., Ferguson, S. J., Eds.; Cambridge University Press: New York, 1988; pp 219−243.
(5) Bock, E.; Koops, H.-P.; Harms, H.; Ahlers, B. In *Variations in Autotrophic Life*; Shively, J. M., Barton, L. L., Eds.; Academic Press: San Diego, CA, 1991; pp 171−200.
(6) Schlegel, H. G. In *Biology of Inorganic Nitrogen and Sulfur*; Bothe, H., Trebst, A., Eds.; Springer-Verlag: New York, 1981; pp 3−12.
(7) *Biological Nitrogen Fixation*; National Academy Press: Washington, DC, 1994; pp 6−32.
(8) Burns, R. C.; Hardy, R. W. F. *Nitrogen Fixation in Bacteria and Higher Plants*; Springer-Verlag: New York, 1975.
(9) Prince, R. C.; George, G. N. *Nat. Struct. Biol.* **1997**, *4*, 247−250.
(10) Igarashi, N.; Moriyama, H.; Fujiwara, T.; Fukumori, Y.; Tanaka, N. *Nat. Struct. Biol.* **1997**, *4*, 276−284.

10.1021/ic048822a CCC: $30.25
Published on Web 12/24/2004

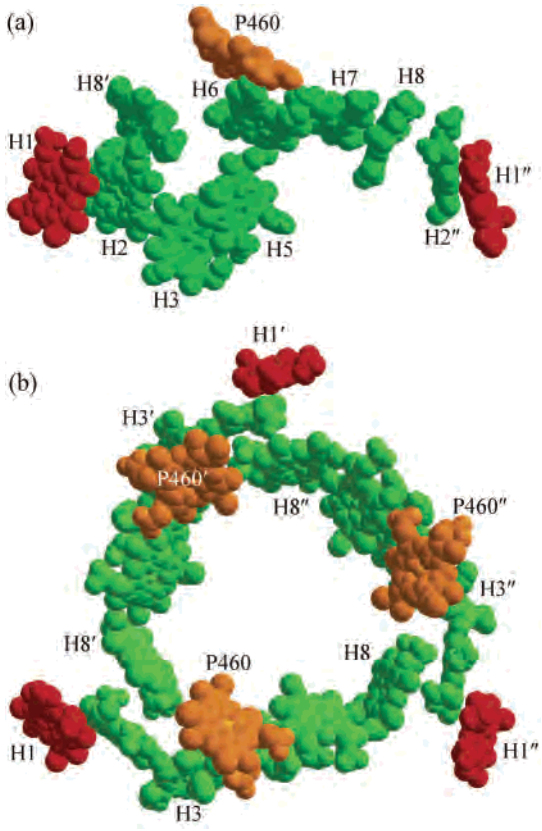

Figure 1. (a) Arrangement of the eight hemes within one subunit of HAO. (b) Arrangement of all the hemes within the HAO trimer; primes are used to distinguish subunits. The hemes are labeled according to the format used by Igarashi et al.,[10] except for P_{460} which was labeled heme 4 in the original article.

pathway. Herein we describe the results obtained using one such technique.

NH_2OH oxidation by HAO takes place on three novel hemes known as P_{460}'s, that have vacant coordination sites at which NH_2OH can bind and be oxidized (Figure 1).[10−14] The remaining 21 HAO hemes are of *c*-type and 6-coordinate, with two axial His ligands each.[10,15] These hemes are low-spin ferric in the resting enzyme, and closely spaced. Hence, they can act as electron transfer agents, accepting the electrons that P_{460} abstracts from NH_2OH.[10,15] Moreover, heme 8 in each subunit lies sufficiently near heme 2 of an adjacent subunit to possibly allow e^- transfer between subunits. Indeed, the 18-heme circle seen in the HAO trimer (Figure 1b) appears to be superbly designed to allow e^- entering at a single P_{460} to be rapidly distributed throughout the trimer. Heme 1 (Figure 1) is the only heme apart from P_{460} that is solvent exposed, and it appears to be the in vivo exit point for the electrons extracted from NH_2OH oxidation. The electrons go from heme 1 to cyt c_{554}, a soluble 26.1 kDa tetra-heme protein[16,17] that is quite abundant in the periplasm of *Nm europaea*,[18] and is now generally recognized to be the acceptor of the electrons from HAO in vivo.

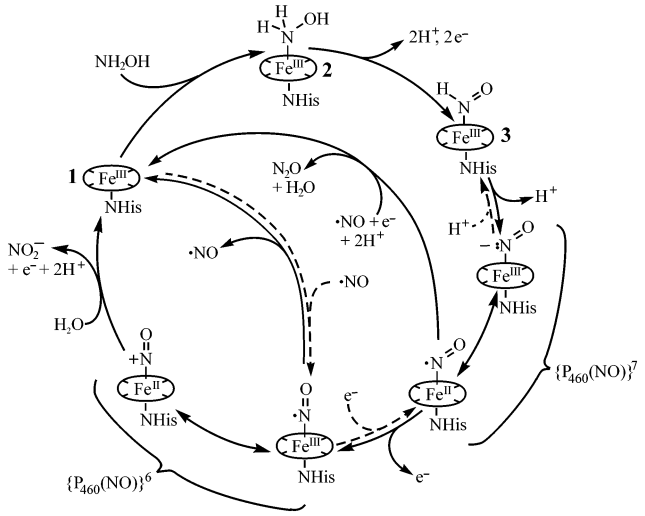

Figure 2. Putative N-containing intermediates generated at the P_{460} active site during catalytic NH_2OH oxidation to NO_2^-. The electrons leaving the P_{460} fragment will be passed on to the HAO *c*-hemes (see Figure 1). N_2O and free $NO^\bullet$ are possible side products, as described in the text.[18] Intermediates containing Fe−NO fragments are each represented in terms of two resonance structures, and of the corresponding Enemark−Feltham description $\{Fe(NO)\}^n$. In this notation, the superscript *n* is the sum of the d electrons that would be counted on Fe if the ligand were actually $NO^\bullet$, and the π^* electron from the $NO^\bullet$.[26] Note that "P_{460}" is used in place of "Fe" in the notation, to emphasize that it is the P_{460} heme that is nitrosylated.

An important goal of our research is to characterize the nitrogen-containing intermediates generated at the P_{460} active site during catalytic NH_2OH oxidation to NO_2^-. On the basis of extensive literature precedent,[19−25] Figure 2 outlines some of the N-containing fragments that are predicted. The figure also introduces a slight modification of the convenient Enemark−Feltham notation, $\{P_{460}(NO)\}^n$, to describe intermediates containing Fe−NO fragments.[26] The likelihood that $\{P_{460}(NO)\}^n$ species are intermediates in the catalytic cycle led us to adopt and extend a methodology for generating such species from free $NO^\bullet$ using a photochemical trigger.[27−30] This method exploits the fact that the water-soluble com-

(11) Hooper, A. B.; Terry, K. R. *Biochemistry* **1977**, *16* (3), 455−459.
(12) Hendrich, M. P.; Logan, M.; Andersson, K. K.; Arciero, D. M.; Lipscomb, J. D.; Hooper, A. B. *J. Am. Chem. Soc.* **1994**, *116*, 11961−11968.
(13) Logan, M. S. P.; Balny, C.; Hooper, A. B. *Biochemistry* **1995**, *34*, 9028−9037.
(14) Logan, M. S. P.; Hooper, A. B. *Biochemistry* **1995**, *34*, 9257−9264.
(15) Arciero, D. M.; Hooper, A. B. *J. Biol. Chem.* **1993**, *268*, 14645−14654.
(16) Iverson, T. M.; Arciero, D. M.; Hsu, B. T.; Logan, M. S. P.; Hooper, A. B.; Rees, D. C. *Nat. Struct. Biol.* **1998**, *5*, 1005−1012.
(17) Andersson, K., K.; Lipscomb, J. D.; Valentine, M.; Munck, E.; Hooper, A. B. *J. Biol. Chem.* **1986**, *261*, 1126−1138.
(18) Whittaker, M.; Bergman, D.; Arciero, D.; Hooper, A. B. *Biochim. Biophys. Acta* **2000**, *1459*, 346−355.
(19) Hoshino, M.; Maeda, M.; Konishi, R.; Seki, H.; Ford, P. C. *J. Am. Chem. Soc.* **1996**, *118*, 5702−5707.
(20) Ford, P. C.; Lorkovic, I. M. *Chem. Rev.* **2002**, *102*, 993−1017.
(21) Wolak, M.; van Eldik, R. *Coord. Chem. Rev.* **2002**, *230*, 263−282.
(22) Fernandez, B. O.; Ford, P. C. *J. Am. Chem. Soc.* **2003**, *125*, 10510−10511.
(23) Choi, I.-K.; Liu, Y.; Wei, Z.; Ryan, M. D. *Inorg. Chem.* **1997**, *36*, 3113−3118.
(24) Feng, D.; Ryan, M. D. *Inorg. Chem.* **1987**, *26*, 2480−2483.
(25) Einsle, O.; Messerschmidt, A.; Huber, R.; Kroneck, P. M. H.; Neese, F. *J. Am. Chem. Soc.* **2002**, *124*, 11737−11745.
(26) Enemark, J. H.; Feltham, R. D. *Coord. Chem. Rev.* **1974**, *13*, 339−406.
(27) Namiki, S.; Arai, T.; Fujimori, K. *J. Am. Chem. Soc.* **1997**, *119*, 3840−3841.
(28) Cabail, M. Z.; Lace, P. J.; Uselding, J.; Pacheco, A. A. *J. Photochem. Photobiol., A* **2002**, *152*, 109−121.
(29) Bodemer, G.; Ellis, L. M.; Lace, P. J.; Mooren, P. E.; Patel, N. K.; Ver Haag, M.; Pacheco, A. A. *J. Photochem. Photobiol., A* **2004**, 53−60.
(30) Moua, V.; Bae, E.; Pacheco, A. A. Manuscript in preparation.

Scheme 1 [a]

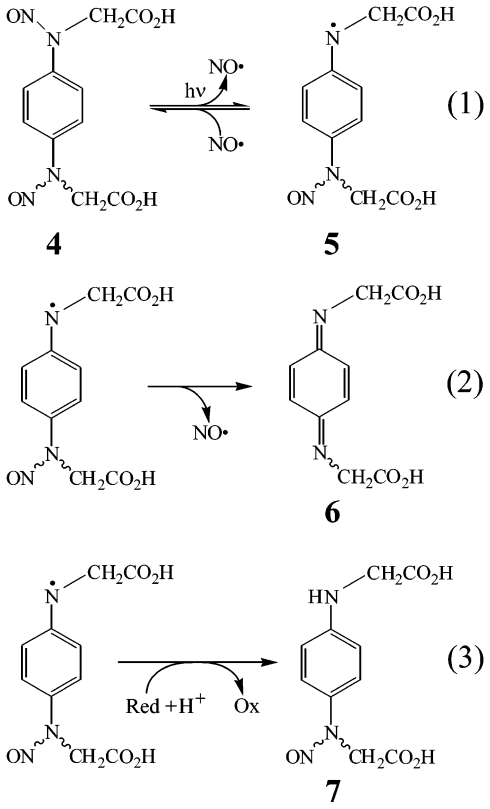

[a] "Red" refers to an arbitrary electron donor.

pound *N*,*N*′-bis(carboxymethyl)-*N*,*N*′-dinitroso-*p*-phenylenediamine (species **4**, Scheme 1) will efficiently generate free NO• upon irradiation with 308 nm light.[27−30] If a XeCl excimer laser is used to initiate the photoreaction, the NO• becomes available on the microsecond to millisecond time scales, and can then be used to nitrosylate the P_{460} active site (dashed arrows, Figure 2).

Scheme 1 describes the NO• generation process. The laser pulse promotes the fragmentation of **4** into **5** and NO• (Scheme 1, eq 1). Species **5** is very reactive and will rapidly recombine with NO•, or fragment further to give the relatively stable species **6** and a second equivalent of NO• (Scheme 1, eq 2).[27,28] Species **5** is also a powerful oxidant, which will be irreversibly reduced to **7** in the presence of a suitable electron donor (Scheme 1, eq 3).[29,30] Thus, species **4** must be used with one of two experimental protocols, depending on the situation. When nitrosylation of a nonreducing species is desired, solutions containing only **4** and the species to be nitrosylated can be irradiated. However, if the species to be nitrosylated is also a reducing agent, then a sacrificial electron donor must be added to the mixture in order to avoid oxidizing the species of interest with **5**.[29,30] We previously reported on the reaction of fully oxidized HAO with photogenerated NO•, which resulted in formation of {Fe(NO)}^{6} (Figure 2) and allowed us to simulate the final reductive nitrosylation steps of the proposed mechanism.[31] These experiments did not require addition of a co-reducing agent.[31] Herein we present the results of exposing HAO reduced by 3-e$^-$/monomer to NO•, photogenerated in the presence of Ru^{II} as co-reductant. The goal of these experiments was to generate the putative 4-e$^-$ reduced intermediate that would be obtained by adding 1 equiv per HAO monomer of NH_2OH to the fully oxidized enzyme (Figure 2).

Experimental Section

Materials. HAO was purified as described in ref 31, the photoactive NO releasing species **4** was synthesized according to the procedure of ref 28, and Ti^{III}(citrate) was prepared as described in ref 32. $[Ru(NH_3)_6]Cl_2$ was obtained from Aldrich. Myoglobin (crystallized and lyophilized horse skeletal muscle) and ferricytochrome *c* (cyt *c*, lyophilized horse heart prepared using TCA) were from Sigma. All other chemicals were from Fisher. Unless otherwise specified, all solutions were made up in 100 mM phosphate buffer, pH = 7.4.

Stock Solution Preparations. Stock solutions of **4**, Ti^{III}(citrate) (Ti^{III}), and $[Ru(NH_3)_6]Cl_2$ (Ru^{II}) were prepared and stored in a nitrogen-filled glovebox. The Ru^{II} stocks were made fresh daily, and stored in a 4 °C fridge until needed. The concentrations of Ru^{II} and Ti^{III} solutions were obtained by monitoring their ability to reduce cyt *c*, using UV−vis spectroscopy.[33] The myoglobin obtained from Sigma was in the fully oxidized "met" state (met-Mb) and was reduced in the glovebox with Ti^{III} prior to use. The reduced myoglobin (Mb) stock solutions used for laser-induced nitrosylation experiments contained 39.2 μM of the protein, and also 146 μM of Ru^{II}. The concentrations of Mb, met-Mb, and cyt *c* solutions were determined directly by UV−vis spectroscopy.[33−35]

The concentration of HAO solutions is reported throughout in terms of subunit concentration, determined from the extinction coefficient at the *c*-heme soret peak of the oxidized enzyme (700 mM^{-1} cm^{-1} at 408 nm).[13] Aliquots (100 μL) of HAO (typically ∼20−40 μM in subunit concentration) were stored in 1 mL cryogenic tubes, in a liquid nitrogen storage vessel. When needed, an uncapped cryogenic tube containing one aliquot of still-frozen HAO was placed in the mini-antechamber of the glovebox, submitted to 4 rapid pump−purge cycles, then brought inside the box still frozen. The tube was recapped and placed in a 4 °C fridge inside the box for ∼60 min. Unless otherwise stated, the following procedure was then used. The HAO aliquot was diluted to 1.5 mL with phosphate buffer, and enough Ru^{II} stock to make the final solution 140 μM in Ru^{II}. This solution was transferred to a cuvette and titrated with Ti^{III}(citrate). The titration was monitored by UV−vis spectroscopy and stopped upon obtaining the absorbance ratios A_{410}/A_{420} = 0.882, and A_{552}/A_{420} = 0.153. Previously, spectropotentiometric titrations revealed that these ratios correspond to HAO in which 3/8 *c*-hemes in each monomer have been reduced.[36]

Laser-Initiated Nitrosylation Experiments. In preparation for most experiments, the following procedure was used. HAO or Mb stock solution (75 μL) was mixed with varying volumes of stock **4** and phosphate buffer, to give solutions with fixed total volumes of 150 μL. These solutions were transferred to 3 mm × 3 mm quartz cuvettes that were then sealed with greased ground glass stoppers. The amount of NO• generated in any given experiment was controlled either by varying [**4**] in the cuvette, or by using

(31) Cabail, M. Z.; Pacheco, A. A. *Inorg. Chem.* **2003**, *42*, 270−272.
(32) Codd, R.; Astashkin, A. V.; Pacheco, A.; Raitsimring, A. M.; Enemark, J. H. *J. Biol. Inorg. Chem.* **2002**, *7*, 338−350.
(33) Margoliash, E.; Frohwirt, N. *Biochem. J.* **1959**, *71*, 570−573.
(34) James, B. R. *Physical Chemistry, Part C*; Dolphin, D., Ed.; The Porphyrins, Vol. V; Academic Press, Inc.: New York, 1978; pp 207−302.
(35) Hoshino, M.; Ozawa, K.; Seki, H.; Ford, P. C. *J. Am. Chem. Soc.* **1993**, *115*, 9568−9575.
(36) Cabail, M. Z.; Pacheco, A. A. Unpublished.

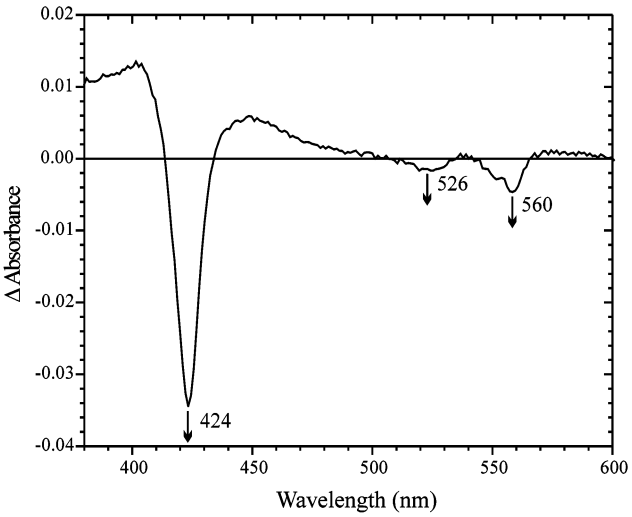

Figure 3. Spectral changes observed 20 ms after photoexcitation of a solution initially containing 68 μM **4**, 70 μM Ru^{II}, and 650 nM HAO, in which 3/8 hemes of each monomer had been prereduced with Ti^{III} citrate. For this experiment, the solution was irradiated in a 2 mm × 10 mm fluorescence cuvette, with the laser pulse traversing the 2 mm width of the cuvette, as described in ref 28.

filters to attenuate the laser pulse and keeping [**4**] constant at 900 μM.[28] In all cases, the [NO•] generated exceeded the amount of HAO nitrosylated by a sufficient amount that, for kinetic analysis, pseudo-first-order conditions prevailed. The amount of NO• produced under a given set of conditions was quantified in separate experiments using excess Mb as a spectroscopically detectable NO• scavenger.[29,35] Full details of these experiments will be presented elsewhere.[30] For HAO nitrosylation experiments in which only small amounts of NO• were generated using attenuated laser pulses, each run was carried out in triplicate, and the results were averaged. In addition, a run with Mb was carried out before and after the three runs with HAO. The [NO•] for the HAO experiments was then taken to be the average of the [NO•] generated in the Mb runs. For HAO nitrosylation experiments in which relatively large amounts of NO• were produced by using the laser at full intensity, the [NO•] generated in each experiment was taken as equal to 20% of the concentration of **4** used in that experiment.[30] In all cases, the average variation in [NO•] generated from one run to the next was ~10%, presumably attributable to variations in the laser pulse intensity.

For the experiment that resulted in Figure 3, the sample preparation method was somewhat different in detail than described above, and laser photolysis was carried out in a 10 mm × 2 mm quartz cuvette, as described in ref 28.

Photochemical fragmentation of species **4** was initiated with a 10 ns, 308 nm pulse from a XeCl excimer laser (TUI, Existar 200). An OLIS RSM-1000 spectrophotometer was used to monitor the absorbance changes induced by the laser pulse. The configuration of the laser and spectrophotometric equipment has been described in general terms elsewhere.[28] Preliminary data were collected with the OLIS RSM-1000 in rapid-scanning mode (scanning slit width = 0.2 mm), which allows complete spectra to be obtained in 1 ms. The preliminary data showed that the reactions of interest had half-lives of less than 0.6 ms, so subsequent experiments were performed with the RSM-1000 in fixed-wavelength mode (fixed middle slit width = 0.6 mm). In this mode, changes in absorbance at a single wavelength could be obtained for time intervals as short as 4 μs. The preliminary multiwavelength data were used to choose an appropriate wavelength to monitor. For both the fixed-wavelength and rapid-scanning experiments, the monochromator entrance slit width was 0.6 mm, and the exit slit width was 0.12 mm. The 418.7 nm band of holmium oxide (IBM Standards 9420) was used as a reference for calibrating the spectrophotometer wavelength in each mode. The data were analyzed using the commercially available software packages Specfit/32, Version 3.0 (Spectrum Software Associates), Microcal Origin, Version 6.0 (Microcal Software, Inc.), and Mathcad11 (Mathsoft Engineering and Education, Inc.).

Results

An investigation that will be presented elsewhere revealed that $[Ru(NH_3)_6]^{2+}$ (Ru^{II}) can reduce the radical species **5** (Scheme 1, eq 3) at diffusion-limited rates ($k = 2 \times 10^9$ M^{-1} s^{-1}).[30] This makes Ru^{II} an ideal candidate for the role of sacrificial electron donor in laser experiments involving photolysis of **4**, because relatively low [Ru^{II}] will be needed to ensure that NO• and the stable species **7** (Scheme 1, eq 3) are obtained quantitatively from **5**. In all the experiments described below, [Ru^{II}] was high enough to remove all traces of species **5** in less than ~20 μs. Figure 3 shows the difference spectrum obtained 20 ms after irradiating a thoroughly anaerobic solution containing **4**, Ru^{II}, and 3-e^- reduced HAO. The Figure 3 difference spectrum is characteristic of *c*-heme oxidation.[37] The prominent negative signal at 424 nm would be seen for any of the HAO *c*-hemes. On the other hand, the signal at 560 nm is unique to heme 3, which is one of two *c*-hemes that have reduction potentials of ~0 mV. This signal has a prominent shoulder at ~552 nm, which is where the remaining *c*-hemes show difference absorbance minima during oxidation.[37] The difference spectrum shows no evidence of spectral changes involving nitrosylation of the P_{460} center, which results in visible spectroscopic characteristics very different from those due to *c*-hemes.[38] However, these spectral changes are often roughly 15 times weaker than corresponding *c*-heme signals,[13,38] so $\{P_{460}(NO)\}^n$ species may be present and not readily detectable (see below).

Figure 4 shows a typical ΔA_{424} versus time trace obtained after irradiating mixtures of **4**, 3-e^- reduced HAO, and Ru^{II} (further examples are given as Supporting Information). The negative signal at 424 nm grows in exponentially from zero, with a rate constant $k_{obs} = 1250 \pm 150$ s^{-1} that is independent of [NO•] generated by the laser pulse (Figure 5), and an amplitude that has hyperbolic dependence on [NO•] (Figure 6). For experiments in which the laser was used at full intensity and [**4**] was <100 μM, an additional very fast drop in A_{424} took place in the dead-time of the instrumentation. This *c*-heme oxidation phase is believed to be initiated by photoexcitation of HAO itself, and is discussed more fully in Supporting Information.

In 3-e^- reduced HAO, the extra electrons reside on two ~0 mV hemes (heme 3 and heme 8, Figure 1), and a high potential heme 2 ($E° = 288$ mV).[37,39,40] The molar absorp-

(37) Collins, M. J.; Arciero, D. M.; Hooper, A. B. *J. Biol. Chem.* **1993**, *268*, 14655−14662.
(38) Hendrich, M. P.; Upadhyay, A. K.; Riga, J.; Arciero, D. M.; Hooper, A. B. *Biochemistry* **2002**, *41*, 4603−4611.
(39) Hendrich, M. P.; Petasis, D.; Arciero, D. M.; Hooper, A. B. *J. Am. Chem. Soc.* **2001**, *123*, 2997−3005.
(40) Kurnikov, I.; Ratner, M. A.; Pacheco, A. A. *Biochemistry* , accepted.

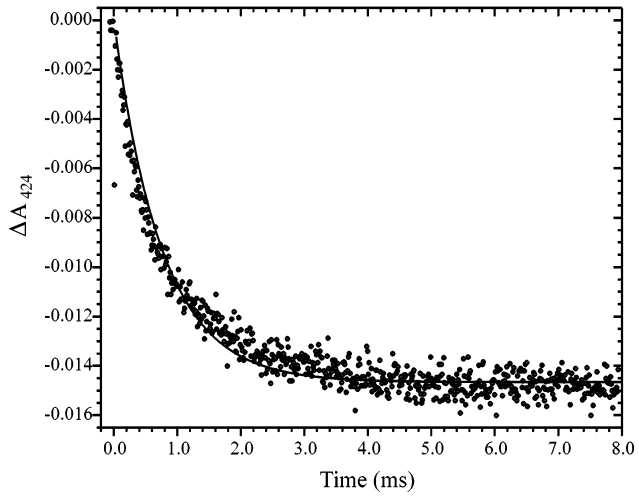

Figure 4. Δ*A* vs time trace obtained at 424 nm, after photoexcitation of a solution initially containing 905 μM **4**, 73 μM Ru^{II}, and 1.04 μM HAO, in which 3/8 hemes of each monomer had been prereduced with Ti^{III} citrate. The solution was irradiated in a 3 mm × 3 mm cuvette. For this experiment, a filter with 44% transmittance was used to attenuate the laser pulse, and [NO•] generated ~10 μM. The data were fitted with an exponential function, $y = A_0 + b[1 - \exp(-k_{obs}t)]$. Other data sets are provided as Supporting Information.

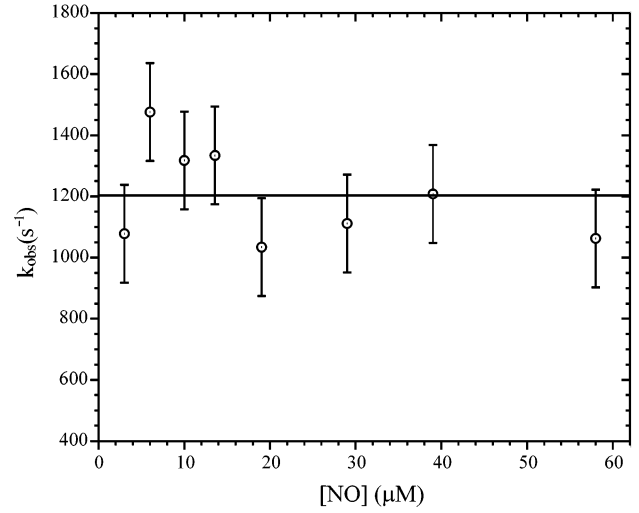

Figure 5. Dependence of the k_{obs} values on [NO•] generated, for a series of experiments analogous to that depicted in Figure 4. The raw data are given as Supporting Information. The horizontal line represents the average k_{obs} (1250 s^{-1}), while the vertical error bars give the standard deviation (±150 s^{-1}).

tivity differences at 424 nm ($\Delta\epsilon_{424}$) associated with oxidation of these hemes are 101 mM^{-1} cm^{-1} for two ~0 mV hemes 3 and 8, and 114 $mM^{-1}cm^{-1}$ for heme 2.[37] Application of Beer's law to the data in Figure 6, using the published $\Delta\epsilon_{424}$ values and the cell path length of 3 mm, shows that roughly one out of three electrons is removed from the *c*-heme pool at sufficiently high [NO•]. Because heme 3 and heme 8 have approximately the same potential, in the resulting 2-e^- *c*-heme system, one of the electron is expected to equilibrate between these two hemes. The fact that the signal with maximal intensity at 560 nm also has a significant shoulder at 552 nm (Figure 3) supports this assumption.

The same reaction that traps the photogenerated NO• (Scheme 1, eq 3) also generates equivalent amounts of

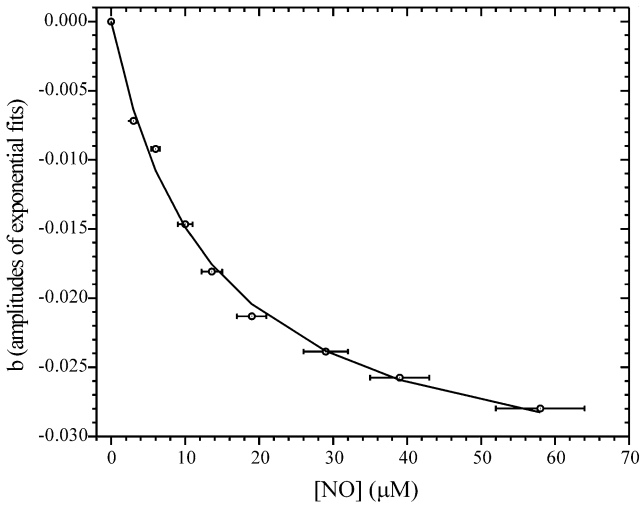

Figure 6. Dependence of the amplitude of the exponential fitting function on [NO•] generated, for a series of experiments analogous to that depicted in Figure 4. The data are fitted to a rectangular hyperbola, $b = b_{max}[NO•]/(K^{-1} + [NO•])$, where the significance of *K* is shown in Scheme 2. The calculated parameters are the following: $b_{max} = -0.035 \pm 0.001$; $K^{-1} = 13 \pm 1$ μM. The raw data are given as Supporting Information.

species **7** and $[Ru(NH_3)_6]^{3+}$ (Ru^{III}). Therefore, an obvious explanation for the observed oxidation of HAO is that Ru^{III} serves as the oxidant. However, the data are not consistent with this explanation. The standard reduction potential for Ru^{III} is 100 mV,[41] and calculations show that even for the lowest amount of Ru^{III} generated (3 μM) the fraction of 0 mV hemes oxidized should have been about 70%. At this [Ru^{III}], the fractional oxidation obtained from Figure 6 is roughly 20%. At the highest concentrations of Ru^{III} generated (60 μM, Figure 6), >99% of the 0 mV hemes should have been oxidized, whereas experimentally the value is less than 45%. This suggests that oxidation of HAO by Ru^{III}, while thermodynamically favorable, is slow and not the reaction observed herein. The independence of the k_{obs} value on [Ru^{III}] (=[NO•], Figure 5) is also inconsistent with [Ru^{III}] being the oxidizing agent in the observed reactions. Oxidation by Ru^{III} would almost certainly take place at the solvent-exposed *c*-heme 1 (Figure 1) via an outer-sphere process, and should have first-order dependence on [Ru^{III}]. Saturation is not expected in an interaction between HAO and a nonphysiological, small oxidant.[42,43]

Scheme 2 presents an alternative hypothesis to explain the observed HAO oxidation, which is that oxidation of the *c*-heme pool is coupled to nitrosylation of the P_{460} active site. According to this hypothesis, NO• first binds to the P_{460} ferric heme to give $\{P_{460}(NO)\}^6$ (Scheme 2, eq 1). This is followed by intramolecular electron transfer (IET) from the 0 mV hemes to P_{460}, which reduces the active site to $\{P_{460}(NO)\}^7$ (Scheme 2, eq 2). Formation of a stable $\{P_{460}(NO)\}^7$ species following an initial nitrosylation step

(41) Bard, A. J.; Faulkner, L. R. *Electrochemical Methods, Fundamentals and Applications*, 2nd ed.; John Wiley and Sons: New York, 2001; p 809. This value was verified in our buffer solution.
(42) Liang, Z.-X.; Nocek, J. M.; Huang, K.; Hayes, R. T.; Kurnikov, I. V.; Beratan, D. M.; Hoffman, B. M. *J. Am. Chem. Soc.* **2002**, *124*, 6849−6859.
(43) Liang, Z. X.; Kurnikov, I. V.; Nocek, J. M.; Mauk, A. G.; Beratan, D. N.; Hoffman, B. M. *J. Am. Chem. Soc.* **2004**, *126*, 2785−2798.

Scheme 2 [a]

$$(Fe^{II}_{(0)})_2P_{460} + \cdot NO \underset{}{\overset{K_1}{\rightleftharpoons}} (Fe^{II}_{(0)})_2\{P_{460}(NO)\}^6 \quad (1)$$

$$(Fe^{II}_{(0)})_2\{P_{460}(NO)\}^6 \underset{}{\overset{K_2}{\rightleftharpoons}} Fe^{II}_{(0)}Fe^{III}_{(0)}\{P_{460}(NO)\}^7 \quad (2)$$

$$(Fe^{II}_{(0)})_2P_{460} + \cdot NO \underset{}{\overset{K}{\rightleftharpoons}} Fe^{II}_{(0)}Fe^{III}_{(0)}\{P_{460}(NO)\}^7 \quad \text{Net}$$

[a] The HAO *c* hemes are labeled with their redox potentials subscripted in brackets.

is consistent with the fact that at most one electron is lost from the HAO *c*-heme pool, irrespective of the amount of Ru(III) or NO• photogenerated (Figure 6).

Discussion

Figure 2 suggests that NH_2OH binds to P_{460} to give species **2**, and is then oxidized and deprotonated to give species **3**. If the reaction begins with HAO fully oxidized, and is carried out in the absence of an external electron acceptor such as cyt c_{554}, then one of the electrons initially removed from **2** will end up on the high potential heme 2, and the other will equilibrate between the two 0 mV hemes (3 and 8).[37,39,40] The subsequent deprotonation step leaves the active site in the $\{P_{460}(NO)\}^7$ state, and HAO overall in the state suggested by Scheme 2 to result from nitrosylating the 3-e^- reduced enzyme. The complete dashed pathway in Figure 2 corresponds to Scheme 2, with a protonation step added. Our experiments do not reveal whether the product of Scheme 2, eq 2, is subsequently protonated. However, they clearly demonstrate that in 4-e^- reduced HAO (as would be obtained by adding 1 equiv of NH_2OH to a fully oxidized enzyme subunit) only two electrons will be transferred to the *c*-heme pool, while the other two will remain on the $P_{460}-NO$ moiety. If Scheme 2, eq 2, did not lie far to the right, then in the nitrosylation experiments the *c*-heme pool should be oxidized by less than 1 equiv, even at saturating [NO•].

The fact that the *c*-heme pool was not oxidized by more than 1 e^-/subunit in the nitrosylation experiments provides excellent evidence that, upon addition of 1 equiv NH_2OH to the fully oxidized enzyme, the first two electrons would be readily transferred to the *c*-heme pool, as proposed in Figure 2. Presumably, these intramolecular electron transfer steps would be coupled to concomitant H^+ transfers. The HAO crystal structure shows that Asp 267 and His 268 are oriented toward the P_{460} active site, and it has been suggested that these residues may contribute to coupled $e^- - H^+$ transfer.[10] Recent papers report the isolation of stable Fe and Ru porphyrin species best formulated as the protonated forms of $\{M(NO)\}^8$ ($\{M(HNO)\}^8$).[44,45] For HAO, such a species would sit between **2** and **3** in Figure 2. In our experiments, the generation of a more highly reduced P_{460} nitrosylation product, such as $\{P_{460}(HNO)\}$,[8] would require the removal of two electrons from the *c*-heme pool. Again, the results show that the *c*-heme pool is reduced by only one electron following nitrosylation, so $\{P_{460}(HNO)\}^8$ is not being generated.

Hendrich et al. recently reported that when 0.48 mM of fully reduced HAO was put under 1 atm NO•, most of the hemes were reoxidized.[38] The lowest potential HAO hemes ($E° < -150$ mV)[37,39] might be capable of reducing NO• back to NH_2OH; however, much of the heme oxidation in these experiments was probably coupled to the reduction of 2 equiv of NO• to N_2O, via the shunt pathway shown in Figure 2. N_2O is the most common product of nonenzymatic NH_2OH oxidation by metals,[46] and significant amounts of N_2O are released in vitro when HAO reacts with NH_2OH.[18,47] N_2O is also produced by *Nm europaea* in vivo, though in this case HAO appears to be one of several sources of the gas.[18,48,49] In our experiments, the limited oxidation of the *c*-heme pool following nitrosylation shows that, with [NO•] of up to 60 μM and on the time scale investigated herein, N_2O is not released from HAO. Such a release would require the concomitant removal of another electron from the *c*-heme pool.

From the hyperbolic fit in Figure 6, one can obtain an equilibrium binding constant $K = (7.7 \pm 0.6) \times 10^4\ M^{-1}$ for the net nitrosylation reaction of Scheme 2. This value is ~5 times higher than that for typical ferriheme proteins such as Mb and Hb ($\sim 1.4 \times 10^4\ M^{-1}$),[19,35] but orders of magnitude smaller than that for the corresponding ferroheme proteins ($\sim 10^{11}\ M^{-1}$).[19] Presumably, the stability of $\{P_{460}(NO)\}^7$ relative to oxidation by the 0 mV *c*-hemes helps to minimize NO• release from the enzyme during turnover, which should be higher from a $\{P_{460}(NO)\}^6$ moiety (but see below). However, excessive stabilization of $\{P_{460}(NO)\}^7$ would trap this moiety and prevent catalysis.

Making the assumption that $K_2 > 10$ (on the basis of the fact that Scheme 2, eq 2, lies far to the right) provides an upper estimate of $\sim 8 \times 10^3\ M^{-1}$ for the value K_1, which governs the formation of $\{P_{460}(NO)\}^6$ from NO• and **1** (Scheme 2, eq 1). This low value suggests that NO• should bind only weakly to fully oxidized HAO, in which stabilization of $\{P_{460}(NO)\}^7$ by IET from the *c*-heme pool is not an option. As mentioned above, NO• normally binds weakly in $\{Fe(NO)\}^6$ hemoproteins,[19,35] and it binds even more weakly in nonprotein $\{Fe(NO)\}^6$ moieties.[50] However, in their recent report Hendrich and co-workers reported obtaining an extremely tenacious $\{P_{460}(NO)\}^6$ species after putting fully oxidized HAO under 1 atm NO•.[38] Indeed, after removing all the free NO• from solution, these workers could only remove the bound NO• by irradiating the solution with intense white light. These results suggest that on a time scale longer than was monitored in our experiments, a protein conformational change can trap NO• in the active site, even

(44) Sulc, F.; Immoos, C. E.; Pervitsky, D.; Farmer, P. J. *J. Am. Chem. Soc.* **2004**, *126*, 1096−1101 and references therein.

(45) Lee, J. Y.; Richter-Addo, G. B. *J. Biol. Inorg. Chem.* **2004**, *98*, 1247−1250.

(46) Wieghardt, K. *Adv. Inorg. Bioinorg. Mech.* **1984**, *3*, 213−274.

(47) Hooper, A. B.; Terry, K. R. *Biochim. Biophys. Acta* **1979**, *571*, 12−20.

(48) Beaumont, H. J. E.; Hommes, N. G.; Sayavedra-Soto, L. A.; Arp, D. J.; Arciero, D. M.; Hooper, A. B.; Westerhoff, H. V.; van Spanning, R. J. M. *J. Bacteriol.* **2002**, *184*, 2557−2560.

(49) Beaumont, H. J. E.; van Schooten, B.; Lens, S. I.; Westerhoff, H. V.; van Spanning, R. J. M. *J. Bacteriol.* **2004**, *186*, 4417−4421.

(50) Ellison, M. K.; Scheidt, W. R. *J. Am. Chem. Soc.* **1999**, *121*, 5210−5219.

as a $\{P_{460}(NO)\}^6$ moiety. Such behavior has precedent in the NO•-transporting nitrophorins,[51,52] in which $\{P_{460}(NO)\}^6$ is stabilized by a major protein conformational change that effectively seals the NO• within the protein. This conformational change is slow relative to initial NO• binding.[51,52]

The fact that the apparent rate constant for nitrosylation (k_{obs}, Figure 5) is independent of [NO•] suggests that even the rapid binding observed in the current study is preceded by a comparatively slow conformational change, which determines the attainable reaction rate. The IET step (Scheme 2, eq 2) could only become rate-limiting at a [NO•] where all of the P_{460} was in the $\{P_{460}(NO)\}^6$ form. On the basis of the arguments of the previous paragraph, such a [NO•] should be fairly high. At present, it is unclear what kind of conformational change would be necessary in order to allow NO• to bind, since the crystal structure appears to show a relatively open P_{460} active site. More studies will be required to address this question. Future experiments are also planned in which higher [NO•] and longer time scales will be monitored, so that the N_2O shunt pathway can be characterized (Figure 2). The fact that HAO nitrosylation and subsequent N_2O formation appear to proceed on very different time scales will greatly simplify investigations of the two processes.

(51) Andersen, J. F.; Ding, X. D.; Balfour, C.; Shokhireva, T. K.; Champagne, D. E.; Walker, F. A.; Montfort, W. R. *Biochemistry* **2000**, *39*, 10118−10131.

(52) Ding, X. D.; Weichsel, A.; Andersen, J. F.; Shokhireva, T. K.; Balfour, C.; Pierik, A. J.; Averill, B. A.; Montfort, W. R.; Walker, F. A. *J. Am. Chem. Soc.* **1999**, *121*, 128−138.

Supporting Information Available: Conditions for all photoinitiated reactions of NO• with 3-e$^-$ reduced HAO (Table S1); all ΔA_{424} vs time traces obtained after irradiating mixtures of **4**, 3-e$^-$ reduced HAO, and Ru^{II} (Figure S1a−h); dependence of A_0 (ΔA_{424} at $t = 0$ from Figure S1a−h) on [NO•] generated (Figure S2); interpretation of this dependence. This material is available free of charge via the Internet at http://pubs.acs.org.

IC048822A